

Ultrastructural analysis of chorion formation in the silkmoth *Bombyx mori*

A. M. PAPANIKOLAOU, L. H. MARGARITIS, AND S. J. HAMODRAKAS

Department of Biochemistry, Cell and Molecular Biology, and Genetics, Athens University, Athens 157.01, Greece

Received February 4, 1985

PAPANIKOLAOU, A. M., L. H. MARGARITIS, and S. J. HAMODRAKAS. 1986. Ultrastructural analysis of chorion formation in the silkmoth *Bombyx mori*. *Can. J. Zool.* **64**: 1158–1173.

The formation of the chorion in the silkmoth *Bombyx mori* (Lepidoptera) is analysed in detail by means of electron microscopy. The secretion of the proteinaceous chorion layers is being accomplished by the follicular epithelial cells which surround the oocyte. The mature chorion exhibits a tripartite ultrastructure; the trabecular layer closest to the oocyte, the inner lamellar layer, and the outer osmiophilic layer. The trabecular layer is deposited first upon the vitelline membrane and further modified possibly by rearrangement and (or) changes of its constituent proteins. A thin porous (sieve) layer is firmly attached to the tips of the follicle cell microvilli and appears to be implicated in the process of secretion of chorion proteins. In early choriogenesis, chorion is a thin (0.7–6 μm) lamellate and simply organized zone becoming thicker (12–20 μm) and more complex as choriogenesis proceeds. Chorion lamellae consist of helicoidally twisted fibrils embedded in an amorphous matrix. A denaturing agent (urea) was used to derive more information concerning assembly of chorion fibrous lamellae. The agent does not seem to eliminate the lamellar organization of chorion although it does modify it. There are suggestions that the agent disrupts many weak interactions, causing conformational changes in the structure of chorion protein components. The surface of the mature chorion is sculptured by follicle cell imprints. Small holes, the aeropyles, which extend radially into chorion down to the trabecular layer presumably serve for respiratory purposes. An elaborate depression in the anterior pole of the chorion, the micropyle, serves for sperm entry.

PAPANIKOLAOU, A. M., L. H. MARGARITIS et S. J. HAMODRAKAS. 1986. Ultrastructural analysis of chorion formation in the silkmoth *Bombyx mori*. *Can. J. Zool.* **64**: 1158–1173.

La microscopie électronique a permis de décrire en détail la formation du chorion chez le ver à soie *Bombyx mori* (Lepidoptera). Les cellules épithéliales folliculaires qui entourent l'ovocyte sont responsables de la sécrétion des couches protéiniques du chorion. Le chorion à maturité a une ultrastructure tripartite: une couche trabéculaire apposée directement à l'ovocyte, une couche lamellaire interne et une couche externe osmiophile. C'est la couche trabéculaire qui se forme d'abord sur la membrane vitelline; cette couche est ensuite modifiée, soit par réarrangement des protéines constitutives, soit par leur modification ou les deux à la fois. Une couche mince et poreuse (filtre) s'attache ensuite solidement aux extrémités des microvillosités des cellules folliculaires; cette couche semble participer au processus de sécrétion des protéines du chorion. Au début de la choriogenèse, le chorion n'est qu'une zone mince (0,7–6 μm) lamellaire à organisation simple mais il devient plus épais (12–20 μm) et plus complexe par la suite. Les lamelles du chorion sont constituées de fibrilles hélicoïdales enfouies dans une matrice amorphe. L'utilisation d'un agent de dénaturation (urée) a permis de connaître plus en détails l'assemblage des lamelles fibreuses du chorion. L'agent ne semble pas éliminer la configuration lamellaire du chorion, bien qu'il en modifie l'organisation. L'agent de dénaturation semble avoir pour effet de rompre plusieurs des "interactions" fragiles, entraînant ainsi des changements dans l'arrangement structural des composantes protéiniques du chorion. La surface du chorion à maturité est sculptée par les empreintes des cellules folliculaires. De petits pores, les aéropyles, creusent le chorion jusqu'à la couche trabéculaire et servent probablement à la respiration. Le micropyle, une dépression complexe au pôle antérieur du chorion, sert à l'entrée du sperme.

[Traduit par la revue]

Introduction

The insect eggshell (vitelline membrane, wax layer, and chorion) (Furnaux and Mackay 1976; Margaritis¹; Margaritis et al. 1980) and the associated follicular epithelium, which secretes its constituent layers, have been the subject of numerous investigations at the cellular and molecular level, providing a model system in several areas of current biological research: physiology of the eggshell layers (Margaritis 1985), control of gene expression in differentiating cells and evolution of multigene families (Regier and Kafatos 1985), morphogenesis of supramolecular structures (Mazur et al. 1980; Smith et al. 1971; Regier et al. 1982), and structural protein folding and organization (Hamodrakas, Asher et al. 1982; Hamodrakas, Jones et al. 1982; Hamodrakas, Paulson et al. 1983; Hamodrakas 1984). Such studies deal largely with the chorion of the silkmoths and in particular with the species *Antheraea polyphemus* (Saturniidae), and *Bombyx mori* (Bombycidae) (Kafatos et al. 1977; Regier et al. 1982; Yamauchi and Yoshitake 1984).

The chorion of the silkmoths is largely proteinaceous; approximately 96% of its dry weight is protein (Kawasaki et al. 1971, 1972). In *B. mori*, more than 150 distinct chorion polypeptides are synthesized and secreted by the follicular cells and deposited around the oocyte, to form the chorion layers (Regier and Kafatos 1985). These proteins have been classified by means of their molecular weights into at least four classes (A, B, C, D), ranging in molecular weight (MW) from 7000 to 30000 (Kafatos et al. 1977). Another class of proteins, called Hc's, are recognized as unique in *B. mori*, on the basis of their unusually high cysteine content. Their molecular weights are mostly D-size, although some are A-, B-, and C-size (Regier and Kafatos 1985).

Fine structural studies have led to the conclusion that silkmoth chorion polypeptides are organized as fibers embedded in a matrix (Regier, Kafatos, Goodfliesh et al. 1978; Regier, Kafatos, Kramer et al. 1978; Hamodrakas, Jones et al. 1982) a feature shared with vertebrate collagenous stroma and other fiber-matrix systems. Comparisons of the protein sequences and predictions of secondary structure (Regier et al. 1983; Regier and Kafatos 1985; Hamodrakas, Jones et al. 1982) have revealed that all chorion proteins have a tripartite structure: a

¹L. H. Margaritis. Choriogenesis in *Drosophila melanogaster*. A model system for the study of cellular differentiation. University of Athens Monograph.

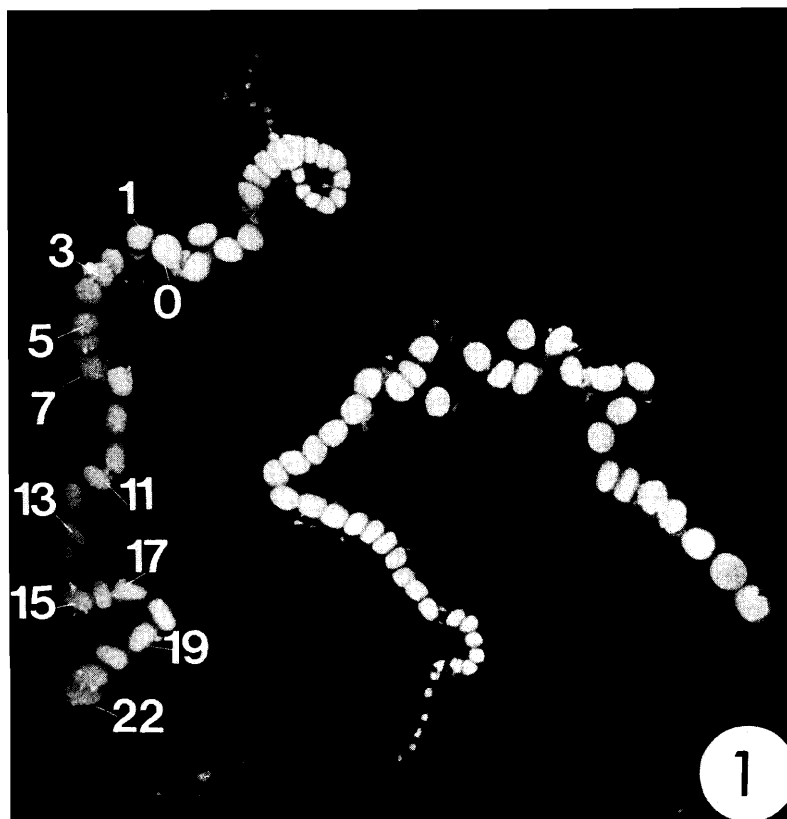


FIG. 1. Two ovarioles dissected from a developing adult female *Bombyx mori*. The paired ovaries in *B. mori* are each composed of four ovarioles. Follicles in progressively advanced stages of development (0, 1, 2, ..., 22) are interconnected in a linear array within each ovariole; number 0 follicle indicates the beginning of choriogenesis. $\times 3.6$.

central, highly conservative and regularly structured domain and two, more variable, flanking arms, particularly enriched in cysteine. In analogy to similar systems of feather and scale keratins, it has been assumed that the central domains form the choriogen fibers, whereas the arms constitute the matrix, presumably serving protein-specific functions (such as cross-linking of the fibers in the late choriogenetic stages, by S—S bonds between cysteines) (Hamodrakas 1984).

Of particular interest is the helicoidal arrangement of the fibers constituting chorion (Mazur et al. 1982; Kafatos et al. 1977; Smith et al. 1971), which suggests structural similarities of the chorion with arthropod cuticle. Bouligand reviewed the occurrence of helicoidal architecture in widely diverse systems such as the crab and locust cuticle, ascidian tunica, and dinoflagellate chromosomes (Bouligand 1972). If the model proposed by Bouligand for the helicoidal architecture is correct, then, the silkworm chorion consists of planes of fibers, roughly parallel to the surface of the oocyte and to each other. In each successive plane, the fiber direction is rotated in a helicoidal manner, through a small angle, about a radial axis perpendicular to the plane of the fibers.

We have undertaken this study (i) to obtain detailed information of choriogenesis in *B. mori* as related to other silkworms; (ii) to attempt useful correlations between chorion structure and assembly, and chorion protein structure, localization, and possible protein structural changes during choriogenesis since a wealth of information has recently been accumulated on *B. mori* chorion protein sequences (Kafatos et al. 1977; Regier and Kafatos 1985; Iatrou et al. 1984).

Materials and methods

Choriogenic follicles were dissected from developing *B. mori* moths (Paul and Kafatos 1975) about 2 days before emergence. According to Nadel and Kafatos (1980), choriogenesis is divided into 26 detailed synthetic stages or 11 abbreviated stages. In the present study, no biochemical determination of choriogenic stages was made; therefore, we were unable to correlate our electron microscopy data with the above mentioned synthetic stages. Thereafter, we shall refer to a certain follicle by declaring its position within the ovariole with respect to the first choriogenic follicle (Kafatos et al. 1977). With this terminology the notation 5/22 means the 5th out of 22 choriogenic follicles in an ovariole (Fig. 1).

Follicles were (i) fixed and processed for transmission and scanning electron microscopy, as described elsewhere (Margaritis et al. 1980), (ii) treated with a urea buffer (0.3 M Tris HCl, pH 8.5, 6 M urea, 1 mM glycine, 1 mM Na₂EDTA) for 60 h and then fixed and processed for thin-section electron microscopy.

Sections were cut with a Sorval MT-1 microtome, stained with uranyl acetate (7%, for 10 min) and lead citrate (0.2–0.4%, for 70 s), and examined in a Philips EM 200 electron microscope operating at 60 kV. Samples for scanning electron microscopy were examined in a Cambridge stereo-scan scanning microscope operating at 25 kV.

Results

Surface view of the chorion

The purified chorion (follicle treated with ethanol to remove the follicle cells and the oocyte) of a nearly mature follicle (22/22) has the shape of a laterally flattened ellipsoid (Fig. 2a) and exhibits anterior–posterior polarity. The three axes are 0.5, 1.1, and 1.4 mm in length. Two planes of symmetry perpendic-

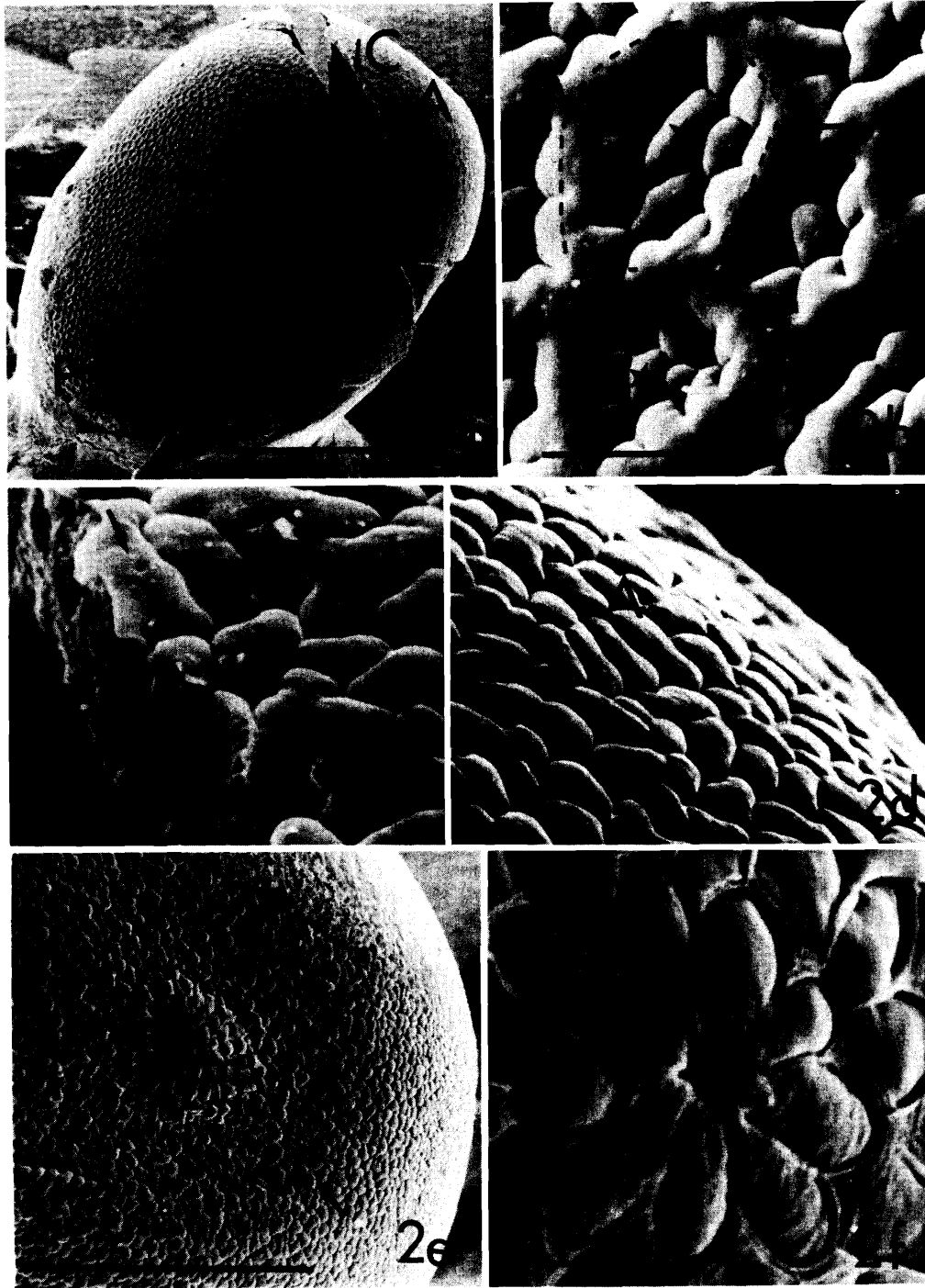


FIG. 2. Scanning electron micrographs of the purified chorion from the late follicle 22/22. (a) There are two planes of symmetry perpendicular to each other, both passing through the longest meridian of the eggshell (one is parallel to the plane of the micrograph). The surface of the chorion shows polyagonal imprints (arrows), each one created by one follicular (epithelial) cell. The anterior pole (A) is slightly flattened. P, posterior pole. C (arrow) indicates a ripped region of the chorion. Bar length is 400 μm . (b) Closer view of the squared region of the chorion surface shown in Fig. 2a. The follicle cell imprints are marked by wide polygonal ridges (dotted lines) which correspond to the intercellular regions of the follicle cells. Several knobs (*) rest within each imprint. Small pores (aeropyles) are seen at the corners of polygons (arrows). Bar length is 20 μm . (c) Side view of the ripped region C of the chorion shown in Fig. 2a. The ridges of the imprints have become flat and the polygons have almost disappeared. The aeropyles (arrows) are seen on the knobs (*). Comparing with Fig. 3a here we have a scanning view of the cross-sectioned chorion. Bar length is 20 μm . (d) Detail of the anterior pole (A) of the chorion. The polygonal imprints have completely disappeared (compare with Fig. 2b). The unfocused region is the chorion dome where the micropyle lies. Bar length is 20 μm . (e) Front view of the micropyle dome (dotted lines). The micropyle (m) is surrounded by four concentric circles of cell imprints. The rest of the surface is covered by knobs (arrows). Bar length is 200 μm . (f) Detail of the micropyle (m arrow) shown in Fig. 2e where the surrounding cell imprints (arrows) take the shape of a rosette. The ridges of the micropyle region are very thin (compare with Fig. 2b) and lack the aeropyles (see also Fig. 2e). The micropyle appears to contain four channels. Bar length is 20 μm .

ular to each other are passing through the long axis of the chorion (Fig. 2a). The chorion surface is marked by a polygonal pattern of wide ridges (Figs. 2a, 2b), not clearly visible in the regions closer to the anterior pole (Figs. 2c, 2d). Every polygon marks the imprint of a single follicle cell since the ridges are formed at the boundaries of adjacent cells (Fig. 2b). Each imprint includes a small number of knobs (1–3) (Fig. 2b), which are formed by the outer layer of the chorion (see also Figs. 3a and 5d).

Tiny holes (the aeropyles) approximately 0.6–0.8 μm in diameter can be observed on the outer surface of chorion, normally at the borders of three-cell imprints (Figs. 2b, 2c).

The anterior pole of chorion contains the micropyle, with the micropylar channels (Yamauchi and Yoshitake 1984) through which sperm entry occurs (Figs. 2e, 2f). The micropyle is bordered by nine central petal-shaped cell imprints which are surrounded by additional (peripheral), elongated imprints gradually merging into the surrounding pattern of polygons (Figs. 2e, 2f). The ridges are lower than in the bulk of the chorion surface (Fig. 2b), substantially narrower, and devoid of aeropyles.

Fine structure of the chorion

A nearly mature follicle (22/22) includes the oocyte surrounded by the vitelline membrane and the chorion. The chorion (Fig. 3a) is approximately 20 μm thick and consists of three main regions: the trabecular layer closest to the oocyte, the inner lamellar layer, and the outer (osmiophilic) layer. The 0.6 μm thick trabecular layer shows fibrous ultrastructure (Fig. 3e). It contains radial columns surrounded by empty spaces, and two spongy layers, a roof and a floor (Fig. 3e). In oblique sections a loose fibrillar material appears to be interconnected with the almost transverse profiles of the columns (Fig. 9g). The thick (approximately 17 μm) inner lamellar layer (ILL) contains 28–30 lamellae which are not uniform in thickness and orientation (Fig. 3a); the first two lamellae closest to the trabecular layer are relatively thin. The next nine lamellae are thinner and randomly oriented. In the middle of the ILL layer five thick lamellae form another sublayer, whereas in the outer part, a fourth sublayer, having the remaining 12–14 lamellae of medium thickness, can be seen (Figs. 3a, 5d). The inner lamellar layer is characterized by many discontinuities and small holes which are more prominent in the inner quarter of the layer (Fig. 3a). The outer osmiophilic layer is deposited late in choriogenesis (Figs. 3b, 3c) and is responsible for the formation of the knobs visible on the surface of the chorion (compare Figs. 2b, 2c, 2d with Figs. 3a, 3b). At this stage, five to six lamellae have already been formed (Figs. 3a, 5d) whereas at least a number of 20–25 lamellae can be observed in a completely mature chorion (data not shown). The lamellae of the outer osmiophilic layer have no discontinuities and they are uniform in thickness ($\sim 0.2 \mu\text{m}$), in contrast to the lamellae of the inner lamellate chorion. In tangential sections to the chorion surface, passing through the osmiophilic knobs, spiral-like configurations can be seen (Fig. 3d) (see also Bouligand 1978). In the center of the spiral the fibrillar ultrastructure of the outer layer is revealed, an array of parallel, thin fibrils. The outer layer is surrounded by the follicular epithelial cells measuring almost half of the chorion thickness (11 μm) (Fig. 3b). A very thin ($\sim 300 \text{ \AA}$, $1 \text{ \AA} = 0.1 \text{ nm}$) sieve layer exists between the microvilli of the follicle cells and the osmiophilic layer (Fig. 3c); this layer is present throughout choriogenesis (Figs. 4a–4f and 5a–5d) and appears as trilaminar (Fig. 3c).

Ultrastructure of the follicles throughout choriogenesis

Follicle 1/22

An early follicle (1/22) consists of the oocyte, the vitelline membrane, the trabecular layer, and the tall columnar follicular cells (28 μm) (Fig. 4a). The floor, columns, and the roof of the trabecular layer (0.3 μm) have already been laid down and they appear to be osmiophilic (Figs. 4a, 9a). Many also osmiophilic, presumably secretory, granules appear within the cytoplasm of the follicular epithelial cells as well as at the extracellular space (Figs. 9a, 4a). In addition many secretory granules are seen to accumulate in the periphery of large cytoplasmic vesicles found mostly, near the secretory surface of the epithelium (Figs. 6a, 6b, 4a).

Follicles 3/22, 5/22, 7/22

A thin 1–3 μm initial framework of the entire inner lamellate chorion has been deposited around the innermost trabecular layer at follicles 3/22, 5/22, and 7/22 (Figs. 1, 4b–4d) (see also Kafatos et al. 1977; Regier et al. 1982). A total of 30 distorted lamellae (bent or curved without breaks) (see also Mazur et al. 1982), can be counted, parallel to the surface of the oocyte. Three to four lamellae in the center of the chorion are 0.2 μm thick, whereas the rest are thinner, approximately 0.1 μm (Figs. 4b–4d). The trabecular layer is not osmiophilic.

Follicles 11/22, 13/22, 15/22

In follicles 11/22, 13/22, and 15/22 the chorion is thicker (12–16 μm) and the trabecular layer measures 0.4–0.6 μm (Figs. 4e, 4f, 5a). Individual lamellae consist of ordered arrays of fibrils (Figs. 8a–8d), whereas many discontinuities and defects are observed in the lamellar organization. The four sublayers of the inner lamellar layer observed in the late follicle 22/22 (see also Figs. 3a or 5d) are very prominent (Figs. 4e, 4f, 5a).

Follicles 17/11, 19/22

In follicles 17/22 and 19/22 the secretion of the osmiophilic layer has already begun (Figs. 5b, 5c, 1). Two to three osmiophilic lamellae can be discerned (Figs. 5b, 5c). This lamellae are always parallel to each other and to the chorion surface, showing very few discontinuities and disruptions. The trabecular layer and the inner lamellar layer maintain their previously documented features.

Follicle 33/33

The osmiophilic layer from a more mature choriogenic follicle (33/33), contains 8–10 lamellae (Fig. 5e). The underlying lamellae (~ 35 in number) of the inner lamellar layer are oriented obliquely with respect to the oocyte surface. Many openings are observed within the inner sublayers of the ILL, whereas holes (0.1–0.3 μm) are scattered mostly in its outermost and middle sublayers (Fig. 5e). The trabecular layer shows a spongy fibrous ultrastructure. In addition, fibers of approximately 30 \AA in diameter are revealed within individual lamellae of the inner lamellar layer, forming characteristic parabolic arcs (Fig. 8f).

Aeropyles

In the first choriogenic follicle (1/22), a bundle of microvilli was seen extending through the follicle cell to the floor of the trabecular layer (Fig. 7a); the long microvilli occur under cell junction regions (Figs. 7a, 7c). As choriogenesis proceeds further, the microvilli become longer and a cylindrical channel forms around them, which is filled with loose flocculent material (Figs. 7b, 7d). Towards the end of choriogenesis,

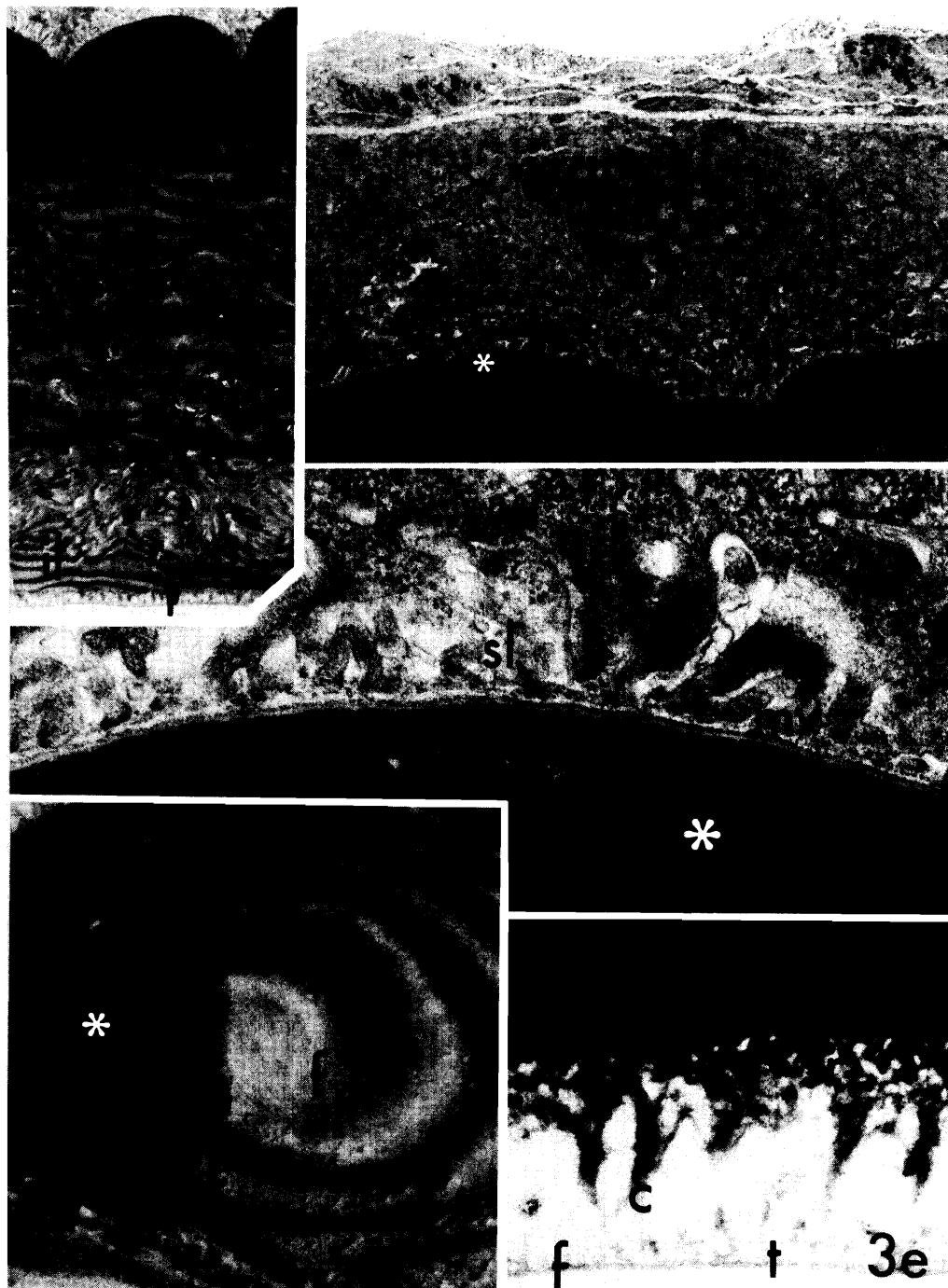


FIG. 3. Transmission electron micrographs of the nearly mature follicle 22/22. (a) Cross section of the chorion. Lying closest to the oocyte is the trabecular layer (*t*) (see also Fig. 3e) and then a thick inner lamellar layer (ILL) followed by an osmiophilic outer layer (*). The ILL can be divided into four sublayers, on the basis of their differences in lamellar thickness and orientation; the innermost sublayer (*il*), consisting of two thin, parallel lamellae close to the trabecular layer; the inner sublayer (*i*), consisting of very thin randomly oriented lamellae; the middle sublayer (*m*), with four to five thick lamellae; and the outermost sublayer (*o*), made up of lamellae of moderate thickness. The bulk of the inner lamellar layer shows many small scattered discontinuities (small arrows) along with small holes (heavy arrows) especially in its inner parts. The outer osmiophilic layer consists of five to six parallel lamellae which are uniform in thickness and show very few or no discontinuities. The osmiophilic layer forms the knobs visible in scanning electron micrographs, in the outer surface of the chorion (see also Figs. 2b, 2c). $\times 4340$. (b) View of the 11 μm thick follicular epithelium (*e*), which is attached to the osmiophilic layer (*). $\times 3100$. (c) Details of the osmiophilic layer (*) and the microvilli (*mv*) of the follicle cells (*e*). In between lies the thin sieve layer (300 \AA), consisting of three minor layers (*sl* arrow). The central layer appears as an electron-dense line ~ 150 \AA thick. $\times 59\ 000$. (d) Spiral arrangement of the osmiophilic layer as seen in a tangential section of a knob (*). Such spirals were also documented by Bouligand (1978) in the crab cuticle. In the center of the spiral the fibrous (*f*) ultrastructure of the osmiophilic layer is revealed. $\times 26\ 000$. (e) Closer view of the trabecular layer (*t*) formed by fibrous columns (*c*) separating two, also fibrous, spongy layers: the roof (*r*) and the floor (*f*). $\times 37\ 000$.

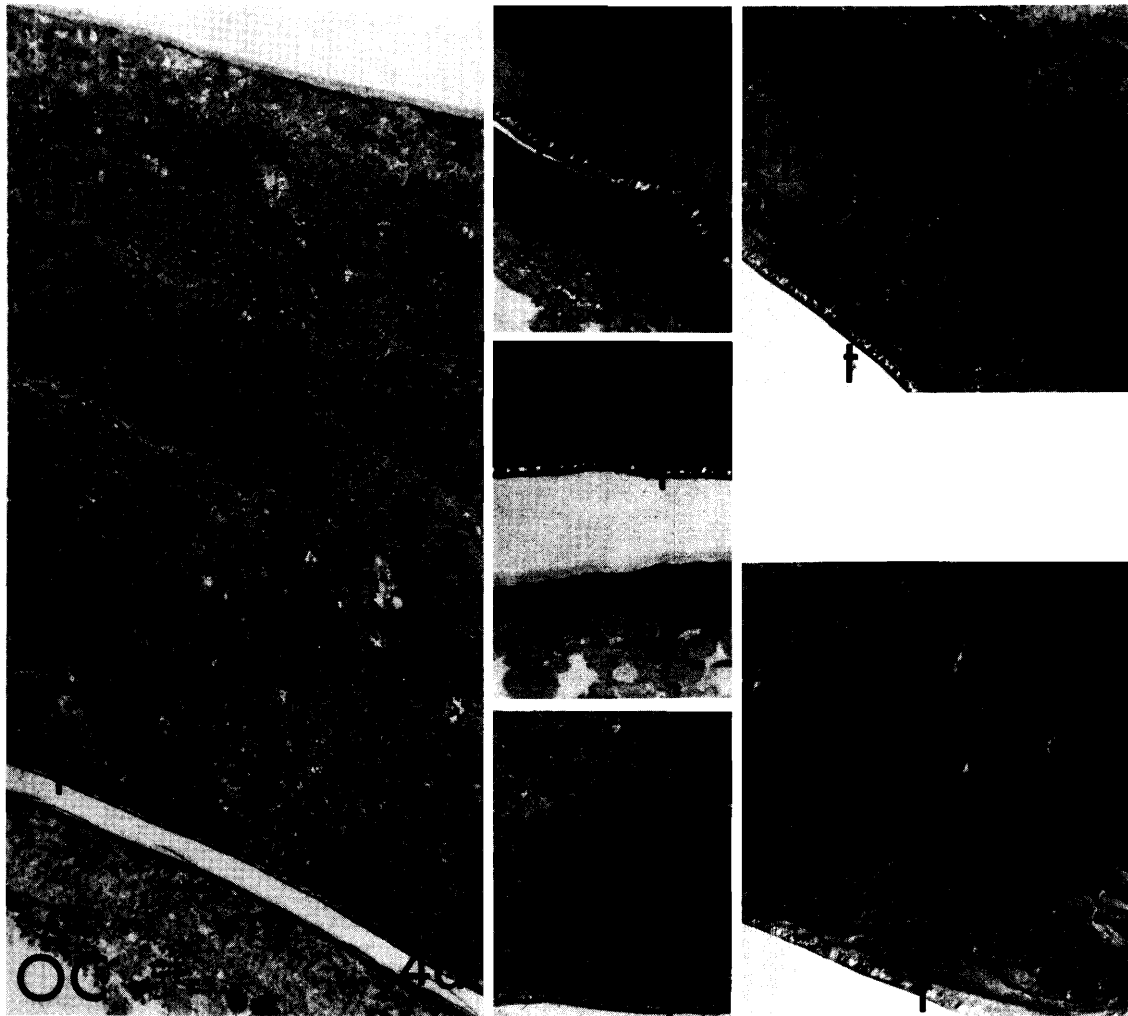


FIG. 4. Transmission electron micrographs showing a series of follicles in different stages of chorion deposition. $\times 3600$. (a) Cross section of the 1/22 follicle. The follicular epithelial cells (*e*), the trabecular layer (*t*) $\sim 0.3 \mu\text{m}$ thick, the vitelline membrane (*vm*), and the oocyte (OC) can be seen sequentially. Many osmiophilic secretory granules (arrows) are scattered throughout the apical cytoplasm of the follicular epithelial cells (see also Figs. 6a, 6b). Observe also the high electron density of the trabecular layer. (b–d) Cross sections of the follicles 3/22, 5/22, and 7/22, respectively. A thin ($1\text{--}3 \mu\text{m}$) lamellate chorion (*ch*) is deposited above the trabecular layer (*t*) which is not electron dense at these follicles. The chorion consists of approximately 30 thin parallel lamellae. Arrows indicate a zone in the middle of the chorion where two to three lamellae are thicker as compared with the rest. (e, f) Cross sections of the follicles 11/22 and 13/22. The chorion is $\sim 13 \mu\text{m}$ thick. The individual lamellae (arrow) consist of helicoidally twisted fibers (see also Figs. 8a–8c), and show various discontinuities and defects. The four sublayers, outer (*o*), middle (*m*), inner (*i*), and innermost (*il*) of the inner lamellar layer are also visible here as described in Fig. 3a. The trabecular layer (*t*), $0.4\text{--}0.6 \mu\text{m}$ thick, is structurally modified (see also Fig. 9c).

localized secretion establishes the external rim of the aeropyle, thus forming a tiny hole within the ridge of a cell imprint (Figs. 2b, 2c). Aeropyles are also formed between the furrows of the knobs of the chorion surface (Fig. 7e) and on the knobs (data not shown, see also Sakaguchi et al. 1973).

Fibrillar ultrastructure of chorion lamellae

The lamellate, early chorion becomes modified during midchoriogenesis; its individual lamellae are made up of thin fibers $80\text{--}110 \text{ \AA}$, which in oblique sections form parabolic arcs (Figs. 8a, 8b, 8d). Each lamella represents a 180° change in the direction of the fibers (Mazur et al. 1982). In a perpendicular section, the lamellae are seen as alternating multiple rows of lines and dots (Fig. 8c). The fibrillar ultrastructure is clearly evident in immature chorions and gradually becomes invisible during the appearance of the osmiophilic layer, first from the

inner part of chorion (Fig. 8e); the fibrillar ultrastructure appears again in the mature chorion (33/33), where fibers seem to have an approximate diameter of 30 \AA (Fig. 8f) (recent data have revealed that the fibrillar ultrastructure characterizes the chorion throughout choriogenesis and after oviposition and fertilization).

The trabecular layer

The trabecular layer is the first chorionic layer formed. While in the first choriogenic follicle 1/22 it has an electron-dense and relatively solid appearance (Fig. 9a), with an approximate thickness of $0.3 \mu\text{m}$, it is substantially modified during choriogenesis; first it becomes less electron dense (Fig. 9b) and then the floor, columns, and roof become spongy and fibrous in texture (Figs. 9c–9g). Its thickness increases to $0.6 \mu\text{m}$ at follicle 22/22 (see Fig. 3e).

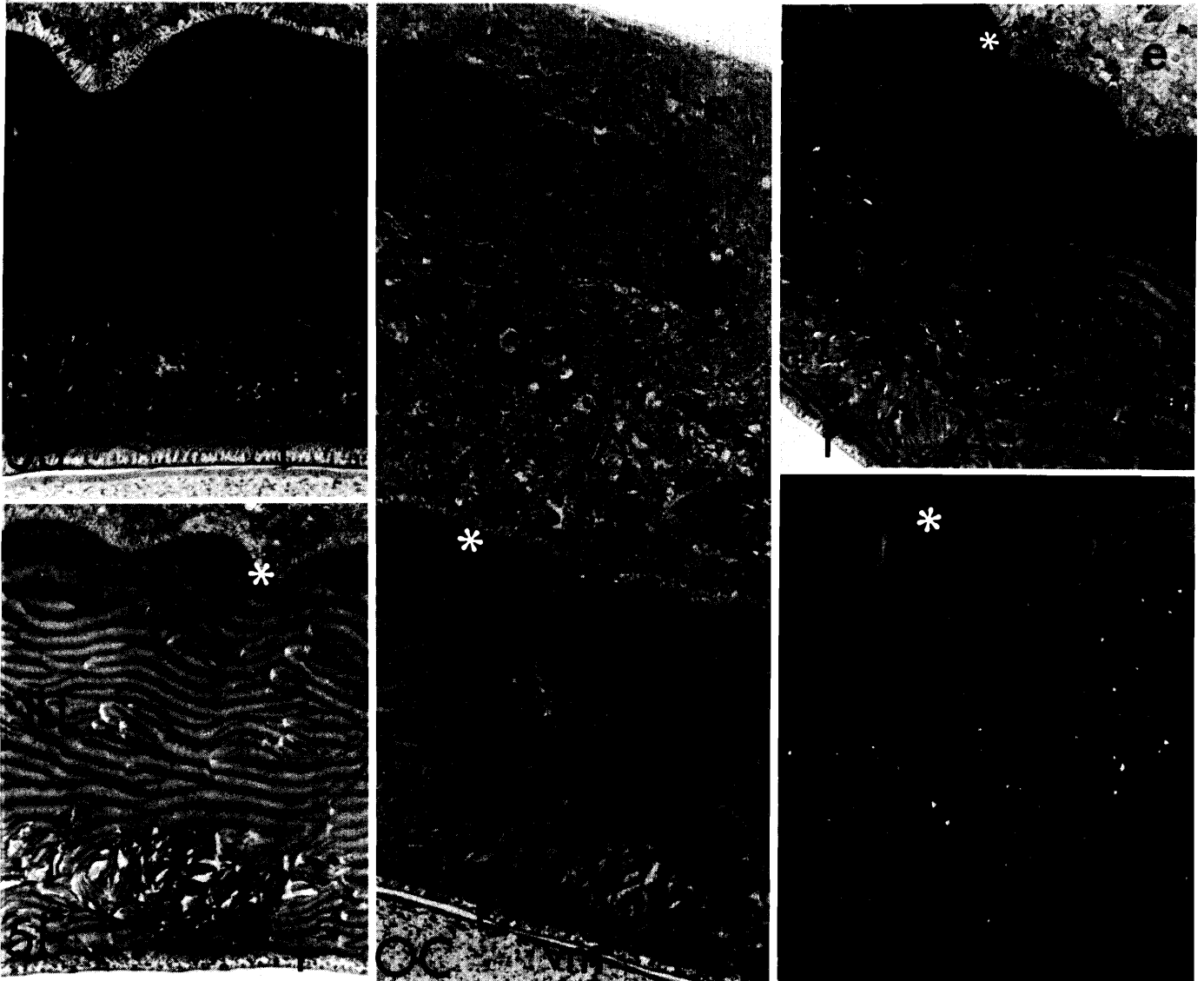


FIG. 5. Cross sections of the chorion of five follicles. $\times 3600$. (a) Cross section of the follicle 15/22. The chorion ($16 \mu\text{m}$ thick) shows almost the same structural features as observed in the chorion of follicle 13/22. *o*, *m*, *i*, *il* are the sublayers of the inner lamellar layer (ILL). The fibrous ultrastructure is still evident within the individual lamellae (see Fig. 8d). The trabecular layer (*t*) is also similar in appearance (see also Figs. 9c, 9d). (b) Cross section of the follicle 17/22. The first lamellae of the outer, extremely electron-dense layer (*) appears, covering the outer surface of the inner lamellar layer (ILL). The fibrillar ultrastructure is obscured in the main bulk of the chorion. However, fibers were still seen in the borders of the ILL with the outer electron-dense (osmiophilic) layer. *t*, trabecular layer. (c) Cross section of the follicle 19/22. The follicular epithelium (*e*) lies above the chorion, which consists of a lamellar osmiophilic layer (*), the inner lamellar layer (ILL), and the trabecular layer (*t*). The oocyte (OC) and the vitelline membrane (*vm*) are also discerned. At this stage, the follicular epithelium is thinner than that observed in the follicle 1/22 (compare with Fig. 4a). (d) Cross section of the follicle 22/22. Symbols have the same meaning as in Fig. 5c. (e) Cross section of the mature choriogenic follicle 33/33. The outer lamellar layer (*) contains 8–10 lamellae. Within each knob (*) lamellae have no discontinuities. The inner lamellar layer (ILL) consists of approximately 35 lamellae which are oriented obliquely with respect to the oocyte surface. Unpublished data show that late as well as laid chorions exhibit a very uniform parallel lamellar packing, parallel to the surface of the oocyte and that in the regions close to the micropyle, lamellae are tilted in a small angle (still remaining parallel to each other), with respect to the oocyte surface. Within the *i* sublayer many openings are observed. Arrows indicate a network of small holes particularly apparent in the outer (*o*) and middle (*m*) sublayers and in the inner (*i*) sublayer. *il*, innermost sublayer; *t*, trabecular layer.

In oblique sections the spongy network of the floor and the roof of the trabecular layer is very prominent (Figs. 9d, 9e), while a loose fibrillar material is seen intervening between the trabecular columns.

Urea-treated chorions

The urea treatment that was applied to the chorions prior to fixation (see Materials and methods) seems to have evoked the rearrangement of the lamellar organization. Electron micrographs

reveal that almost all the lamellae of the chorion have been oriented parallel to the chorion surface in different choriogenic follicles (follicles 19/38, 26/38, 38/38; Figs. 10a–10d).

The high degree of order of the lamellar organization is disrupted by distortions particularly in the outer regions, screw dislocations, and vacancies between individual lamellae (Figs. 10a–10d, see also Mazur et al. 1982). However, the osmiophilic layer remains rather intact against urea treatment (data not shown).

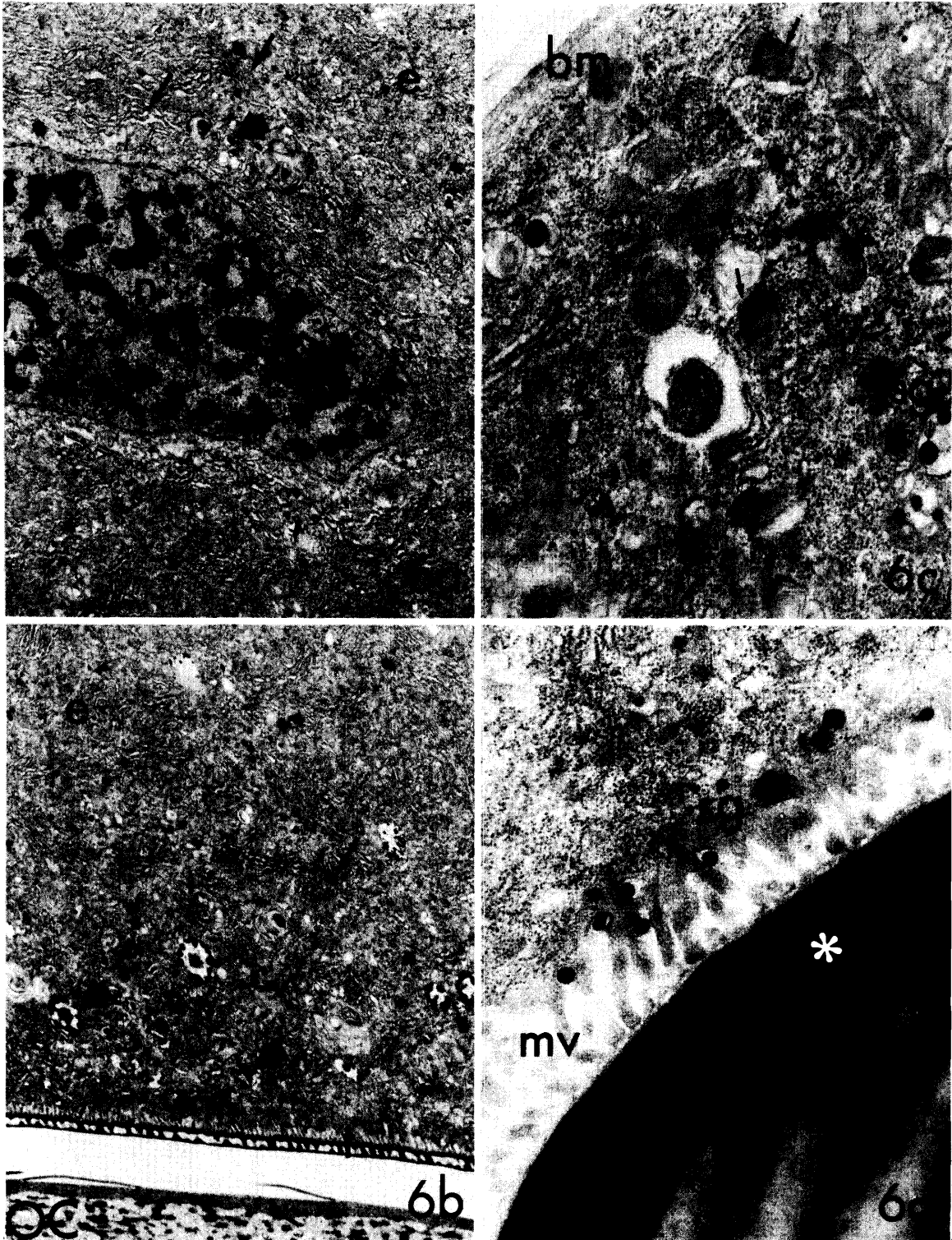


FIG. 6. (a, b) Transmission electron micrographs of thin sections cut through a follicle cell (*e*) (follicle 19/22), showing (a) its nucleus (*n*) and (b) the cytoplasm close to the secretory region. The high synthetic activity of the cell is apparent by the abundance of RER and Golgi complexes (arrows) and also by the osmiophilic secretory granules (heavy arrows) in its cytoplasm. *t*, trabecular layer, OC, oocyte. $\times 10\ 000$. (c, d) Transmission electron micrographs of thin sections cut through a follicle cell (follicle 19/22) showing (c) part of its cytoplasm close to the basal membrane (*bm*) and (d) part of its cytoplasm near the outer surface of the chorion. Secretory granules (*sg*) full of osmiophilic material are seen between, near, or within the microvilli (*mv*) and also close to the basal membrane. A large number of mitochondria (thin arrows) RER membranes and ribosomes are also seen in the cytoplasm. *, osmiophilic layer. $\times 26\ 000$.

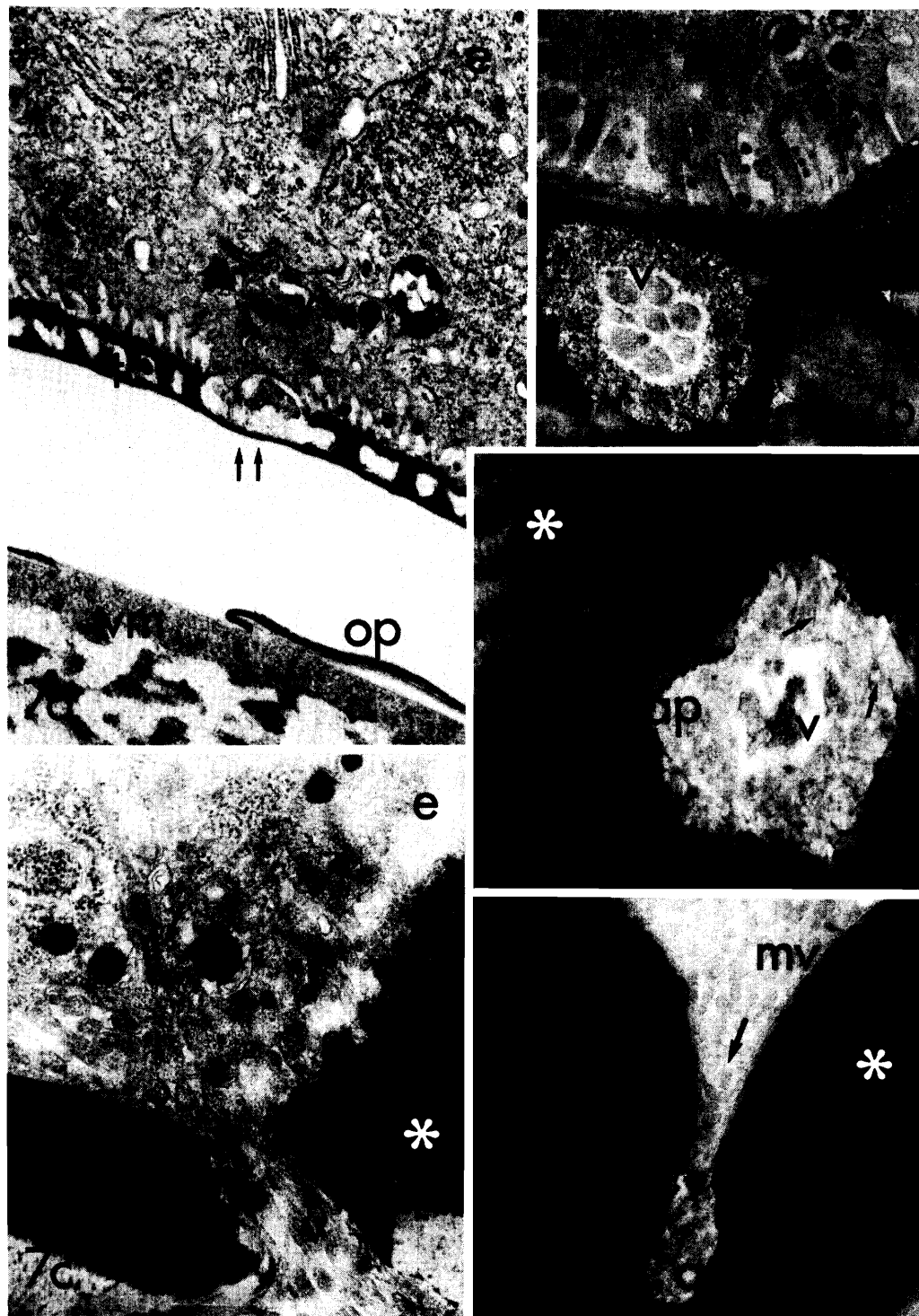


FIG. 7. (a) Transmission electron micrograph of an early stage of choriogenesis (follicle 1/22) showing the formation of an aeropyle. The aeropyle channel (arrows) forms around a bundle of extended microvilli, under a cell junction (heavy arrow), during the formation of the trabecular layer (*t*). *e*, follicle cell; *vm*, vitelline membrane; *op*, overlapping plates of the vitelline membrane. $\times 29\ 000$. (b) Electron micrograph of a thin cross section cut through an aeropyle channel in the outer chorion of follicle 15/22. The extended villi (*v*), which are used as a mold for the formation of the channel, are closely packed and surrounded by a loose fibrous matrix (*f*, filler). *e*, follicle cell. $\times 32\ 000$. (c) Thin section of the top of an aeropyle of 19/22 follicle. A bundle of microvilli (*v*) is transverse both the disrupted sieve layer and the osmiophilic layer (*) forming the basis for a future air channel. The aeropyle is formed under a cell-junction (arrow) of the follicular epithelium (*e*). $\times 35\ 000$. (d) Thin section of an aeropyle (*ap*) right under the osmiophilic layer (*) of follicle 22/22. Inside the villi (*v*) of the channel, numerous cytoplasmic ribosomes can be resolved. Note also the loose fibers (arrows) of the channel filler. $\times 34\ 000$. (e) A micrograph indicating that the furrow (arrow) between the osmiophilic knobs (*) of the outer surface of the chorion is a site where an aeropyle (*ap*) is formed. *mv*, microvilli (follicle 21/22). $\times 24\ 000$.

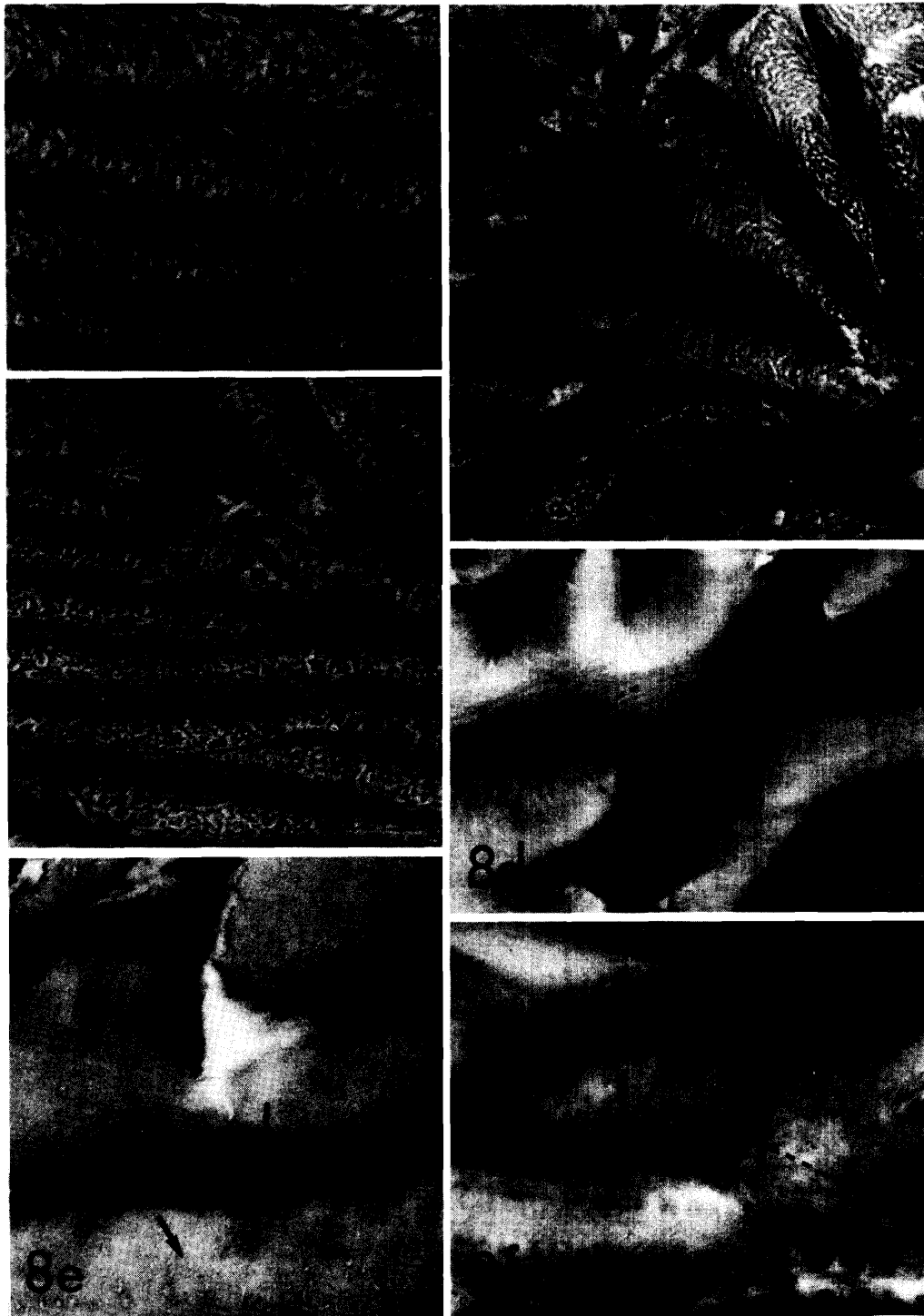


FIG. 8. Transmission electron micrographs of thin sections cut through the chorion, showing the fibrous ultrastructure of its lamellae. (a) The parabolic pattern of fibers ($\sim 110 \text{ \AA}$) (dotted lines) within each lamella (*l*) in an oblique section of follicle 11/22 is shown. $\times 45\ 000$. (b, c) Fibrous lamellae (*l*) in oblique (b) and vertical (with respect to the surface of chorion) sections (c) of the 13/22 chorion. In Fig. 8c the parabolic arcs have disappeared; in the lamellar boundaries, fibers cut longitudinally are seen as parallel lines (arrows) in contrast to those, in the center, cut transversely which are seen as dots (small circles). $\times 45\ 000$. (d) A micrograph showing the inner lamellar layer (ILL) of the chorion of follicle 15/22. Fibers of $\sim 90 \text{ \AA}$ in diameter form parabolic arcs within individual lamellae (dotted lines). $\times 22\ 000$. (e) Micrograph of the inner part of chorion (follicle 19/22) where the fibrous ultrastructure is obscured. Arrows show fibrillar remnants of the chorion lamellae. $\times 47\ 000$. (f) In the mature chorion of the follicle 33/33, fibers of approximately $30\text{--}40 \text{ \AA}$ in diameter can be seen. The dotted lines show the arrangement of the parabolic arcs of fibers within one lamella (*l*). $\times 45\ 000$.

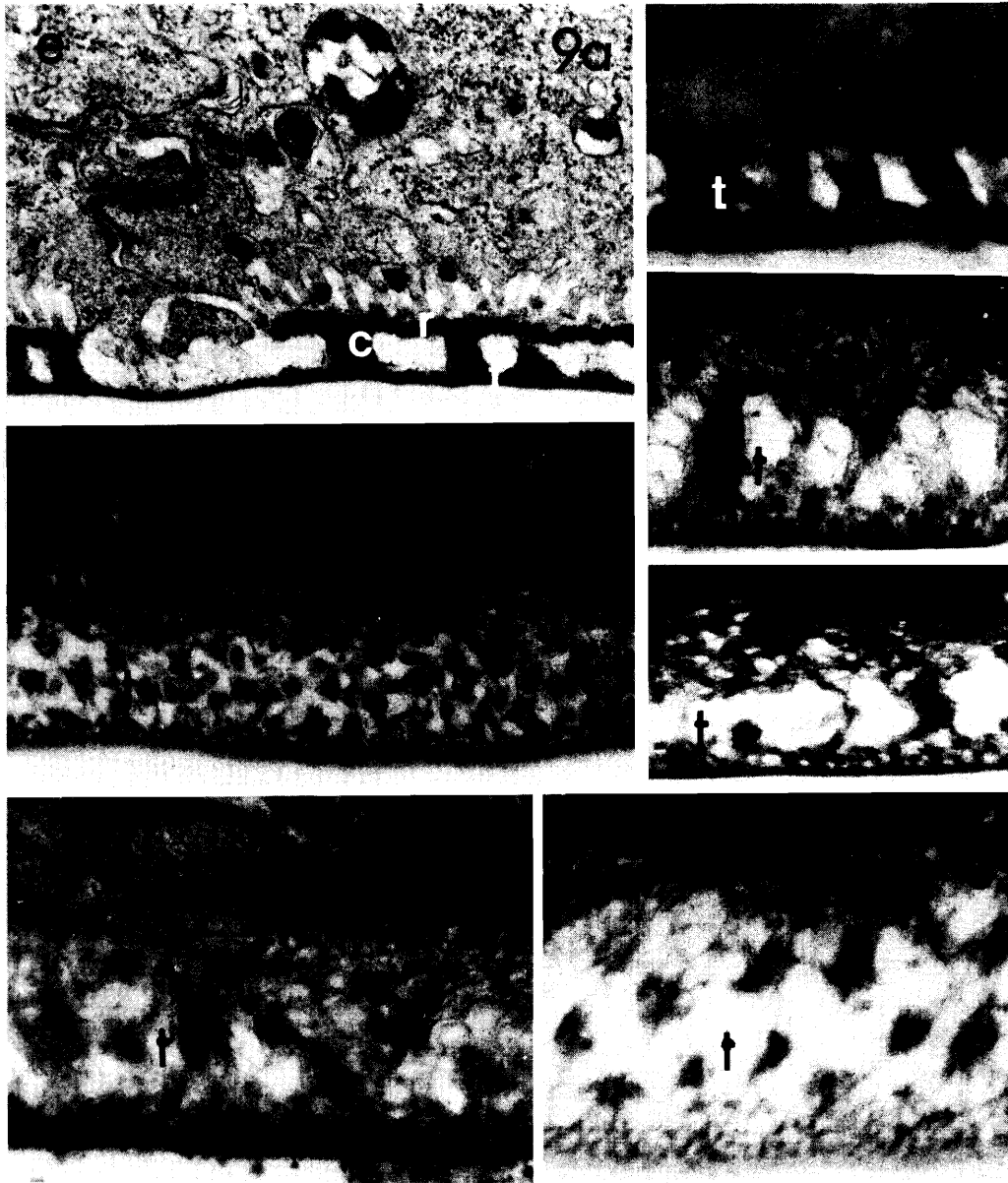


FIG. 9. Transmission electron micrographs of sections cut through the trabecular layer from several follicles. (a) Follicle 1/22. The electron-dense roof (*r*), floor (*f*), and columns (*c*) exhibit a rather solid texture. *e*, follicle cells. $\times 45\ 000$. (b) Follicle 3/22. The trabecular layer (*t*) is no longer osmiophilic but still relatively solid. $\times 45\ 000$. (c, d) Longitudinal (*c*) and oblique (*d*) sections of 15/22 follicle showing the spongy fibrous texture of the trabecular layer (*t*). Compare with Figs. 9a, 9b. In Fig. 9d the columns are cut almost transversely and are interconnected by a loose fibrillar material (see also Fig. 9g). Fig. 9c, $\times 45\ 000$; Fig. 9d, $\times 22\ 000$. (e, f) Cross section (*e*) from the 17/22 follicle and oblique section (*f*) from the 13/22 follicle. The trabecular layer (*t*) has not changed in ultrastructure but only in thickness; it measures $\sim 0.5\ \mu\text{m}$ in the 17/22 follicle. In Fig. 9f the fibrous lamellae (*l*) of chorion are seen attached to the trabecular roof. $\times 45\ 000$. (g) Oblique section of the 22/22 follicle trabecular layer (*t*). The almost transverse profiles of the columns exhibit thin fibrous connections. $\times 45\ 000$.

The fibrillar ultrastructure of chorion, of certain choriogenic follicles, is resolved more clearly after the urea buffer treatment (Figs. 10c, 10d). Figures 10c and 10d highlight the difference between lamellae cut transversely and obliquely, respectively. Finally, the treatment causes loosening of the flocculent texture of the trabecular layer (Figs. 10e–10g).

Discussion

Sequential events during chorion formation

Chorion formation entails sequential events which lead to the creation of a series of specialized layers (Figs. 5d, 5e) by the follicular epithelium. The innermost trabecular layer is deposited first, and then follows the secretion of an initial lamellar

framework of the predominant (in terms of space occupancy) inner lamellar layer (see also Regier et al. 1982). This framework seems to include early features of the later matured inner lamellar layer, a scaffold upon which this layer builds its complexity. By midchoriogenesis the entire lamellate chorion is composed of helicoidally oriented fibrils and lamellae show many discontinuities and defects. The four distinct layers (innermost, inner, middle, and outer) of the inner lamellar layer are already recognized. The last chorion (osmiophilic) layer is deposited late, lamella per lamella (Figs. 5b, 5c, 5d). The thin perforated, trilaminar sieve layer is seen attached to the microvilli of the follicle cells throughout choriogenesis. While chorion maturation proceeds in parallel with gradual obscure-

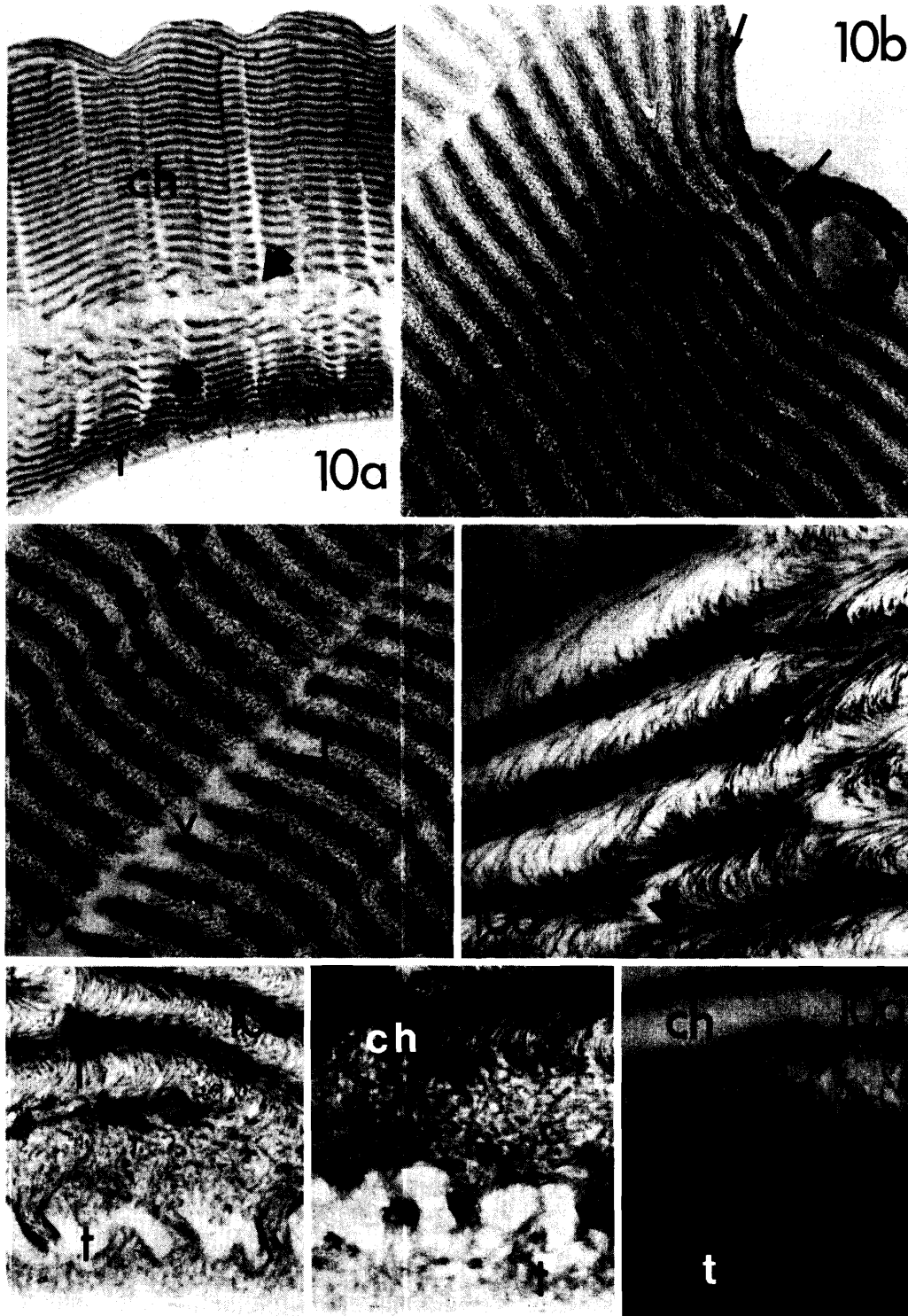


FIG. 10. Transmission electron micrographs of thin sections cut through the chorion from a number of follicles treated with a denaturing agent (see Materials and methods). (a) Low power survey field of the chorion (*ch*) of follicle 19/38. Note the parallel arrangement of the lamellae and the vacancies (arrows) between them. The trabecular layer (*t*) has changed into a more perforated layer (see also Fig. 10e). $\times 3000$. (b) The outer part of the same chorion at higher magnification reveals an empty aeropyle (*ap*) and a screw dislocation (*s*) (see also Mazur et al. 1982) within the lamellar organization (*l*). Note also the 180° change in the orientation of the parabolic patterns of fibers within individual lamellae, in certain chorion regions (arrows). $\times 15\,600$. (c) Image of the inner part of chorion shown in Fig. 10a, illustrating in detail the lamellar organization. The parallel arrangement of the lamellae (*l*) and their fibrous ultrastructure is evident. *d*, arrow and *v* indicate a distortion and a vacancy in the lamellar organization, respectively. $\times 17\,000$. (d) Fibrous ultrastructure of chorion from follicle 26/38. Thin individual fibers (~ 130 Å) (*f*, arrow) are clearly resolved, forming parabolic arcs (dotted lines). In several cases fibers of adjacent lamellae seem to overlap (heavy arrows). $\times 29\,600$. (e) Image of the trabecular layer (*t*) of the same follicle shown in Fig. 10a. The agent causes a loosening of the texture of this layer but it does not disrupt its general structure. The fibrous lamellae (*l*) of the inner lamellar layer are also seen. $\times 32\,800$. (f) Image of the trabecular layer (*t*) of the follicle of Fig. 10d, which is also affected by the agent (urea buffer), showing a looser texture. *ch*, chorion. $\times 32\,800$. (g) Image of the trabecular layer (*t*) of the follicle 38/38. Note that the inner part of chorion (*ch*) shows no fibrillar ultrastructure despite the treatment (compare with Figs. 10e, 10f). $\times 27\,200$.

ment of the fibrillar ultrastructure, thin fibrils are observed to dominate in the late chorion of follicle 33/33 (this will be discussed below).

According to Regier and co-workers (1982) the chorion formation in the Saturniid *Antheraea polyphemus*, is accomplished by two types of mechanisms; one type is apposition and corresponds to secreted material deposited in an outward direction, progressively away from the oocyte and the second is intercalation, in which occurs deep permeation of newly synthesized proteins into the chorion (sieve layer seems to play a very important role in the formation of the lamellae). Whether these types of mechanisms operate in *B. mori* is not known as yet, although recently accumulated information through the analysis of mutants in *B. mori* support the above theory (Nadel et al. 1980).

Follicle cells

The follicular epithelium is very active during chorion formation. It is observed that the chorion precursors (in the secretory granules) are more electron dense than the chorion's structure itself (except during the secretion of the early trabecular and the osmiophilic layer). The change of staining density implies either a change of polypeptide structure (Furnaux and Mackay 1976) or a dissolution of the proteins. The massive concentrations of rough-surfaced endoplasmic reticulum (RER) and Golgi complexes in the follicle cells is concomitant with high protein synthetic activity. Blau and Kafatos (1978) in *A. polyphemus*, have shown that the secretory pathway of proteins involves sequentially the RER, the Golgi apparatus, and finally the secretory granules. Our data show that the RER and Golgi complexes are dispersed in contrast to the highly polarized direction of secretion, possibly due to largely needed cytoplasmic volume for protein synthesis. The high activity of follicle cells seen in late choriogenic stages (Fig. 6c, 6d) is presumably expected since the secretion of the outer, dense osmiophilic layer takes place.

We were unable to explain why the secretory granules accumulate in the vesicles observed near the apical surface of the epithelium, in the early follicle 1/22, although this might be explained with a difference in secretory material which is most likely to occur.

The decrease in height of the epithelium between the various stages is expected, since it is accompanied by a simultaneous increase of chorion volume, and also by the use of the intracellular material to synthesize the chorionic proteins. Finally at ovulation the epithelium is stripped off the chorion surface and left within the ovariole, resulting in the exposure of the surface details.

Aeropyle morphogenesis

Electron micrographs of early follicles show that the future localization of an aeropyle is predetermined, and that its formation begins simultaneously with chorion formation (see Fig. 7a). Microvilli are used as a mold around which a cylindrical channel is built, filled with material (filler). A similar mechanism is documented in *Hyalophora cecropia* by Smith et al. (1971). It is most likely that the filler plays an important role in the aeropyle formation, since in *A. polyphemus* it is incorporated in both aeropyle and aeropyle crowns morphogenesis (Mazur et al. 1980).

From our data and from others (Sakaguchi et al. 1973), aeropyles are not only formed at regions corresponding to three cell junctions (Figs. 7a, 7c, 2b), but also in the furrow between the knobs and on the knobs of the chorion (see Figs. 7e, 2c). The

positioning of aeropyles is genetically controlled and many differences occur within individual mutants of *B. mori* (Sakaguchi et al. 1973).

Chorion assembly and crucial changes of its components

From the present work and from others (Smith et al. 1971; Mazur et al. 1982), it appears that the helicoidal (cholesteric-like) architecture of the chorion of *B. mori* and related silkmoths arises by self-assembly of its constituent protein molecules. The follicle cells do not play a direct role in this process (Smith et al. 1971), since self-assembly is taking place extracellularly; (i) the proteins are considered to be organized to form the three dimensional structure of the chorion at some distance from the points of their secretion (Smith et al. 1971) and, (ii) secreted protein molecules pass through the porous sieve layer to reach their destination: this ensures minimum follicle cell involvement in the self-assembly process.

Helicoidal structures, like cholesteric liquid crystals or cholesteric liquid crystal analogues in biological systems, can be formed by self-assembly of asymmetric and rodlike components (Smith et al. 1971; Bouligand 1975). We have recently proposed that the molecular conformation of silkmoth chorion proteins, which dictates the helicoidal architecture of chorion, is a helical, rodlike structure, the β -pleated sheet (Hamodrakas 1984). We are currently working out the mechanisms of the self-assembly procedure (S. J. Hamodrakas, unpublished data) which apparently, is based on the simple rules of packing of twisted β -pleated sheets (Chothia et al. 1977).

Dramatic changes are seen to occur in the texture of chorion throughout choriogenesis (Figs. 4, 5) (for an exact definition of the term texture see Bouligand 1975). The origin of the different patterns of lamellae and their defects and distortions (the texture) can be visualized as being due to two types of mechanisms which are not mutually exclusive (Mazur et al. 1982). The first is primarily mechanical; preexisting structures might impose boundary conditions on fibrillar direction or lamellar nucleation, and changing shapes of the cellular secretory surface or changing amounts of secreted nonlamellar material might also affect the geometry of the lamellar chorion. The second major cause of pattern variation is the nature and concentration of the chorion proteins present, which depend on the temporally and spatially changing patterns of chorion gene expression. A third mechanism, which is perhaps dependent on the above two, might be based on (i) changes of the molecular conformation of chorion proteins; it is very difficult to predict where and how these changes occur, possibly they are conformational changes of the chorion protein arms, which are rich in Gly (Hamodrakas, Jones et al. 1982; Hamodrakas 1984), since the central, conservative domains of chorion proteins adopt most probably a unique, well-defined structure (S. J. Hamodrakas, unpublished), and (or), (b) alternative ways of efficient packing of chorion proteins.

In this context, it is rather important to note the uniformity of the texture of the outer lamellar layer of chorion, which uniquely appears in *B. mori* (Figs. 5d, 5e). This layer consists of proteins extremely rich in Cys (over 30% in MW, Kafatos et al. 1977; Iatrou et al. 1984) and is formed towards the end of choriogenesis. One wonders whether this uniformity and the lack of defects and distortions is a consequence of the possibility that protein members of the classes Hc-A and Hc-B, which form the outer lamellar layer, are structurally equivalent; it is known that each class consists of several protein members, of apparently different molecular weight (Rodakis et al. 1984). These proteins

are highly homologous in the central conservative domains with members of the A and B classes constituting the main bulk of the chorion, but their arms may adopt very similar three dimensional structures, since they consist of tandem repeats, of variant length, of the dipeptide Cys–Gly, in contrast to the arms of the members of the A and B families, which apparently are more diverse in sequence, length, and perhaps in structure (Iatrou et al. 1984).

Another possible explanation is that the uniformity of texture of the outer lamellar layer arises from the existence of disulfide bonds which cross-link its constituent Hc-A and Hc-B proteins (Hamodrakas 1984). It is perhaps worth noting that towards the end of choriogenesis when chorion is strengthened by the formation of disulfide bonds, its texture appears to be more uniform (Fig. 5e).

The trabecular layer undergoes substantial modification of its structure during choriogenesis (Figs. 9a–9g). By and large, this layer is formed by molecules belonging to the C class of proteins which are minor components of the chorion (Kafatos et al. 1977). These proteins are secreted during the very early stages of choriogenesis and also towards its end (Regier and Kafatos 1985). Although they are similar in terms of sequence and structure in their central conservative domains with the A and B proteins (Regier et al. 1983; G. C. Rodakis and R. Lecanidou, unpublished) they substantially differ in the sequence (and perhaps structure) of their arms, which, in addition, are of much greater length. It is possible that, the apparent changes of the ultrastructure of the trabecular layer during choriogenesis are directly related to changes of conformation of these arms and (or) to changes of protein composition and concentration (Regier et al. 1982).

From the electron micrographs (Figs. 10a–10d) it is obvious that the urea extraction does not eliminate the lamellar organization of chorion although it does modify it. The lamellae exhibit a uniform pattern throughout the chorion, which is devoid of a large number of defects and distortions, as appearing in the chorion under normal circumstances.

At the same time it is clear that the fibrous ultrastructure of the chorion remains a characteristic feature of its architecture (Figs. 10c, 10d). Alterations in the structure of the fibers cannot be discerned at this resolution.

We suggest that the elimination of a large number of defects and distortions is due to the fact that the use of the denaturing agent partially at least, evokes conformational changes in the structure of the chorion protein components, disrupting weak interactions. Such conformational changes may lead to the elimination of considerable strains caused by the exact packing of chorion protein molecules and their spatial organization; this might eventually cause the overall macroscopic softening of the chorion, and the uniform packing of its component lamellae. The patterns of the fibrils in the lamellae do not change, which suggests that the helicoidal (cholesteric-like) architecture of chorion remains intact.

The uniform appearance of lamellae, furthermore, suggests that there is a uniform packing density of protein molecules in the lamellae, since the thickness of a lamella is inversely proportional to the concentration of its constituent molecules (Robinson 1958).

The outer osmiophilic layer remains intact after urea extraction (data not shown), which perhaps is a consequence of the fact that its component protein molecules are cross-linked and stabilized by strong covalent S—S bonds (Hamodrakas 1984), which render this layer unaffected by the denaturing agent.

One puzzling observation, which we believe requires further investigation is the fact that helicoidally organized fibrils appear early in choriogenesis, then occasionally disappear and later reappear as thinner fibrils (30–40 Å) (Figs. 8a–8f).

In the chorions of *A. polyphemus* and *H. cecropia* other investigators (Smith et al. 1971; Regier et al. 1982) have observed that at a certain stage of development, fibrils disappear and they were unable to observe fibrils at the late periods of choriogenesis. The disappearance of the fibrils was attributed to an impregnating matrix material secreted by the follicle cells which obscures the appearance of chorion fibrils. However, our results (together with recent unpublished data) suggest that fibrils are discerned throughout choriogenesis; they appear even in laid eggs. Nevertheless, we are unable to offer a plausible explanation for the change in the thickness of the fibrils, which appears to occur at a certain stage of choriogenesis (towards its end). One attractive hypothesis is that the change in thickness is possibly due to a molecular rearrangement (perhaps the formation of the S—S bonds), which causes the apparent change of the fibrillar thickness. However, this remains to be tested by more refined work and biochemical experiments.

Comparative ultrastructure

Some interesting comparisons can be made between the structure of *B. mori* chorions and those of the two related species *A. polyphemus* (Regier et al. 1980, 1982; Mazur et al. 1980, 1982; Kafatos et al. 1977) and *H. cecropia* (Smith et al. 1971). The chorions of *A. polyphemus* and *H. cecropia* consist of two ultrastructurally distinct layers, the trabecular and the lamellate layers (Smith et al. 1971; Regier et al. 1982). In contrast, *B. mori* chorions contain a third outer, dense osmiophilic layer which presumably gives additional properties to the chorion such as rigidity, impermeability, and resistance (Margaritis 1985). The usefulness of this layer can be easily explained since *B. mori* eggs undergo prolonged periods of diapause, while *H. cecropia* and *A. polyphemus* diapause only as pupae and show very rapidly developing embryos (Kafatos et al. 1977). Other structural differences may reflect other differences in physiology. The trabecular layer in *B. mori* consists of floor columns and a roof; the latter is absent in *H. cecropia* and *A. polyphemus*, where the columns are attached directly to the lamellate chorion. The existence of a perforator roof increases the effective volume occupied by air available at the trabecular layer. This may cause larger quantities of air to be stored and diffused to the oocyte of *B. mori* follicles. In the lamellar region (~20 µm) of *B. mori* chorions the holes (aeropyles) and the cavities are fewer in number and narrower than in *A. polyphemus* and *H. cecropia*. This results in limited water loss but, however, adequate ventilation (Margaritis 1985). *Hyalophora cecropia* chorion, being twice as thick (60 µm) as *A. polyphemus* chorion and needing more air spaces for its ventilation, exhibits large, radial air channels along with small irregular channels (Smith et al. 1971).

Despite the structural differences observed, some very important similarities do exist among the three species. We refer to the existence of the sieve layer, the helicoidal twisted fibrous composition of chorion, and the similar morphogenetic mechanisms of chorion sublayers and regions. These similarities can be attributed to evolutionary conserved mechanisms and structures.

When looking at the outer surface of the chorions of the three species, we can conclude that in *A. polyphemus* there are found four spatially differentiated surface regions (aeropyle crown,

flat, stripe, and micropyle) (Regier et al. 1980) and only the micropyle region is common with *B. mori*. Both species have polygonal ridges on the surface of the chorion, but in *A. polyphemus* they are (in the flat region) wider, double, and have a slight depression in the midline, which corresponds to a two-cell junction; in the stripe region they appear to be missing (also in the aeropyle crowns region), or displaced, as is also observed in the anterior pole of *B. mori* chorion (see Figs. 2c, 2d). *Bombyx mori* has rounded ridges with bulbous mounds (knobs) filling the cell imprints in contrast to *A. polyphemus*. In *A. polyphemus* the aeropyle channels are wide (2 μm) and have tall crowns in the aeropyle crown region, a type of air-capturing plastron aiding respiration during periods of aquatic submergence (Hinton 1970; Margaritis 1985). In *B. mori* the aeropyle channels are smaller (0.6–0.8 μm) and there are no crowns. The aeropyles are situated in places of the ridges, corresponding to three-cell junctions (as in *A. polyphemus*) and in other places too (e.g., between the furrow of the knobs) (see also Sakaguchi et al. 1973). The long diapause of *B. mori* eggs matches very well with the very narrow aeropyles (limited water loss) as compared with the wide aeropyles of *A. polyphemus*. *Hyalophora cecropia* lacks the polygonal network of ridges, stripe, and aeropyle crowns, but shows aeropyles comparable to those of flat region of *A. polyphemus* (Mazur et al. 1980).

The micropyle region is more or less similar in appearance (evolutionary conserved) in both *A. polyphemus* and *B. mori* with a rosette of cell imprints surrounding the micropylar complex of channels. In *A. polyphemus* the micropyle contains nine channels (Regier et al. 1980), while in *B. mori* usually three or four with a range from two to six per egg (Yamauchi and Yoshitake 1984). The number of the available micropylar channels can be related to polyspermy, a usual phenomenon in *B. mori* eggs (Tazima 1978) and other insect eggs (Counce 1972). The micropyle depression lies on a dome in the central front of the anterior pole of the *B. mori* egg and this might facilitate approach and sperm entry (micropyle is set close to the outlet of the spermatheca at oviposition (Omura 1938)). The micropyle region of the chorion lacks trabecular and osmiophilic layers which suggests high specificity.

Acknowledgements

We thank the Greek Ministry of Research and Technology and the University of Athens for financial support.

- BLAU, H. M., and F. C. KAFATOS. 1978. Secretory kinetics in the follicular cells of silkworms during eggshell formation. *J. Cell Biol.* **78**: 131–151.
- BOULIGAND, Y. 1972. Twisted fibrous arrangements in biological materials and cholesteric mesophases. *Tissue Cell*, **4**: 189–217.
- . 1975. Defects and textures in cholesteric analogues given by some biological systems. *J. Phys. Colloq.* **36**: 173–331.
- . 1978. Liquid crystalline order in biological materials. In *Liquid crystalline order in polymers*. Edited by A. Blumstein. Academic Press, New York, San Francisco, London. pp. 261–297.
- CHOTHIA, C., M. LEVITT, and D. RICHARDSON. 1977. Structure of proteins. Packing of α -helices and pleated sheets. *Proc. Natl. Acad. Sci. U.S.A.* **74**: 4130–4134.
- COUNCE, S. J. 1972. The causal analysis of insect embryogenesis. In *Developmental systems: insects*. Vol. 2. Edited by S. J. Counce and C. H. Waddington. Academic Press, New York. pp. 1–156.
- FURNEAUX, P. J. S., and A. L. MACKAY. 1976. The composition, structure and formation of the chorion and the vitelline membrane of the insect eggshell. In *The Insect integument*. Edited by H. R. Hepburn. Elsevier Scientific Publishing Company, Amsterdam. pp. 157–176.
- HAMODRAKAS, S. J. 1984. Twisted β -pleated sheet: the molecular conformation which possibly dictates the formation of the helicoidal architecture of several proteinaceous eggshells. *Int. J. Biol. Macromol.* **6**: 51–53.
- HAMODRAKAS, S. J., S. A. ASHER, G. D. MAZUR, J. C. REGIER, and F. C. KAFATOS. 1982. Laser Raman studies of protein conformation in the silkworm chorion. *Biochim. Biophys. Acta*, **703**: 216–222.
- HAMODRAKAS, S. J., C. W. JONES, and F. C. KAFATOS. 1982. Secondary structure predictions for silkworm chorion proteins. *Biochim. Biophys. Acta*, **700**: 42–51.
- HAMODRAKAS, S. J., J. R. PAULSON, G. C. RODAKIS, and F. C. KAFATOS. 1983. X-ray diffraction studies of a silkworm chorion. *Int. J. Biol. Macromol.* **5**: 149–153.
- HINTON, H. E. 1970. Insect eggshells. *Sci. Am.* **223**(2): 84–91.
- IATROU, K., S. G. TSITILOU, and F. C. KAFATOS. 1984. DNA sequence transfer between two high-cysteine chorion gene families in *Bombyx mori*. *Proc. Natl. Acad. Sci. U.S.A.* **81**: 4452–4456.
- KAFATOS, F. C., J. C. REGIER, G. D. MAZUR, M. R. NADEL, H. M. BLAU, W. H. PETRI, A. R. WYMAN, R. E. GELINAS, P. B. MOORE, M. PAUL, A. EFSTRATIADIS, J. N. VOURNAKIS, M. R. GOLDSMITH, J. R. HUNSLEY, B. BAKER, J. NARDI, and M. KOEHLER. 1977. The eggshell of insects: differentiation-specific proteins and the control of their synthesis and accumulation during development. In *Results and problems in cell differentiation*. Vol. 8. Edited by W. Beerman. Springer-Verlag, Berlin. pp. 45–145.
- KAWASAKI, H., H. SATO, and M. SUZUKI. 1971. Structural proteins in the silkworm eggshells. *Insect Biochem.* **1**: 130–148.
- . 1972. Structural proteins in the eggshells of silkworms, *Bombyx madarina* and *Antheraea mylita*. *Insect Biochem.* **2**: 53–57.
- MARGARITIS, L. H. 1985. Structure and physiology of the eggshell. In *Comprehensive insect biochemistry, physiology and pharmacology*. Vol. 1. Edited by L. I. Gilbert and G. A. Kerkut. Pergamon Press, Oxford and New York. pp. 153–230.
- MARGARITIS, L. H., F. C. KAFATOS, and W. H. PETRI. 1980. The eggshell of *Drosophila melanogaster*. I. Fine structure of the layers and regions of the wild-type eggshell. *J. Cell Sci.* **43**: 1–35.
- MAZUR, G. D., J. C. REGIER, and F. C. KAFATOS. 1980. The silkworm chorion: morphogenesis of surface structures and its relations to synthesis of specific proteins. *Dev. Biol.* **76**: 305–321.
- . 1982. Order and defects in the silkworm chorion, a biological analogue of a cholesteric liquid crystal. In *Insect ultrastructure*. Vol. 1. Edited by H. Akai and P. C. King. Plenum Press, New York. pp. 150–185.
- NADEL, M. R., M. R. GOLDSMITH, J. GOPLERUD, and F. C. KAFATOS. 1980. Specific protein synthesis in cellular differentiation. V. A secretory defect of chorion formation in the Gr^{col} mutant of *Bombyx mori*. *Dev. Biol.* **75**: 41–58.
- NADEL, M. R., and F. C. KAFATOS. 1980. Specific protein synthesis in cellular differentiation. IV. The chorion proteins of *Bombyx mori* and their program of synthesis. *Dev. Biol.* **75**: 26–40.
- OMURA, S. 1938. Structure and function of the female genital system of *Bombyx mori* with special reference to the mechanism of fertilization. *J. Fac. Agric. Hokkaido Imp. Univ.* **40**: 111–128.
- PAUL, M., and F. C. KAFATOS. 1975. Specific protein synthesis in cellular differentiation. II. The program of protein synthetic changes during chorion formation by silkworm follicles, and its implementation in organ culture. *Dev. Biol.* **42**: 141–159.
- REGIER, J. C., and F. C. KAFATOS. 1985. Molecular aspects of chorion formation. In *Comprehensive insect biochemistry, physiology and pharmacology*. Vol. 1. Edited by L. I. Gilbert and G. A. Kerkut. Pergamon Press, Oxford and New York. pp. 113–151.
- REGIER, J. C., F. C. KAFATOS, R. GOODFLIESCH, and L. HOOD. 1978. Silkworm chorion proteins: sequence analysis of the products of a multigene family. *Proc. Natl. Acad. Sci. U.S.A.* **75**: 309–394.
- REGIER, J. C., F. C. KAFATOS, and S. J. HAMODRAKAS. 1983. Silkworm chorion multigene families constitute a superfamily: comparison of C and B family sequences. *Proc. Natl. Acad. Sci. U.S.A.* **80**: 1043–1047.

- REGIER, J. C., F. C. KAFATOS, K. J. KRAMER, R. L. HEINRIKSON, and P. S. KEIM. 1978. Silkmooth chorion proteins: their diversity, amino acid composition, and the NH₂-terminal sequence of one component. *J. Biol. Chem.* **253**: 1305–1314.
- REGIER, J. C., G. D. MAZUR, and F. C. KAFATOS. 1980. The silkmooth chorion: morphological and biochemical characterization of four surface regions. *Dev. Biol.* **76**: 286–304.
- REGIER, J. C., G. D. MAZUR, F. C. KAFATOS, and M. PAUL. 1982. Morphogenesis of silkmooth chorion: initial framework formation and its relations to synthesis of specific proteins. *Dev. Biol.* **92**: 159–174.
- ROBINSON, C. 1958. Surface structures in liquid crystals. *In* Surface phenomena in chemistry and biology. Pergamon Press, London.
- RODAKIS, G. C., R. LECANIDOU, and T. H. EICKBUSH. 1984. Diversity in a chorion multigene family created by tandem duplications and a putative gene-conversion event. *J. Mol. Evol.* **20**: 265–273.
- SAKAGUCHI, B., H. CHIKUSHI, and H. DOIRA. 1973. Observations of the eggshell structures controlled by gene action in *Bombyx mori*. *J. Fac. Agric., Kyushu Univ.* **18**: 53–62.
- SMITH, D. S., W. H. TELFER, and A. C. NEVILLE. 1971. Fine structure of the chorion of a moth *Hyalophora cecropia*. *Tissue Cell*, **3**: 477–498.
- TAZIMA, Y. 1978. The silkworm: an important laboratory tool. Tokyo, Kodansha.
- YAMAUCHI, H., and N. YOSHITAKE. 1984. Formation and ultrastructure of the micropylar apparatus in *Bombyx mori* ovarian follicles. *J. Morphol.* **179**: 47–58.